National Aeronautics and Space Administration

Langley Research Center

Hampton, Virginia 23681-2199

Cloud – Aerosol LIDAR and Infrared Pathfinder Satellite Observations (CALIPSO)

Data Description and Quality Summary

Imaging Infrared Radiometer Level 2 Swath Data

DOI: https://doi.org/10.5067/IIR/CALIPSO/CAL_IIR_L2-Swath_Data_Description_Document_V5

Cloud – Aerosol LIDAR and Infrared Pathfinder Satellite Observations

Data Description and Quality Summary

Imaging Infrared Radiometer Level 2 Swath Data

Primary Authors

Anne Garnier

Analytical Mechanics Associates (AMA)

21 Enterprise Parkway, Hampton, Virginia 23666

Jacques Pelon

LATMOS/IPSL, Université Pierre et Marie Curie

75252 Paris Cedex 5 (France)

Mark Vaughan, Michael Pitts, Charles Trepte, David Winker, Brian Getzewich, Jason Tackett

NASA Langley Research Center

Hampton, Virginia 23681-2199

Jayanta Kar, Kam-Pui Lee

Analytical Mechanics Associates (AMA)

21 Enterprise Parkway, Hampton, Virginia 23666

Timothy Murray, Sharon Rodier

ADNET Systems, Inc.

6720B Rockledge Drive, Suite #504, Bethesda, Maryland 20817

Robert Ryan

Coherent Applications, Inc. – Psionic LLC

1100 Exploration Way, Hampton, Virginia 23666

January 16, 2026

CALIPSO IIR Level 2 Swath Data Description Document
Version 5.00

Data Version:	5.00
Data Release Date:	October 01, 2025
Data Date Range:	June 13, 2006 to June 30, 2023

Introduction

The Infrared Imaging Radiometer (IIR) Level 2 swath data product contains data assigned to 1-km IIR pixels on a 69-km wide grid centered on the CALIPSO lidar (CALIOP) track.

This product includes brightness temperatures measured in the three IIR channels (8.65, 10.60, and 12.05 µm).

The other primary variables, namely a scene classification, effective emissivity in each IIR channel, cloud effective diameter (D_e), and ice or liquid water path are retrieved under the CALIOP track and propagated to the IIR swath using radiative homogeneity criteria (Garnier et al., 2012). For pixels outside the track, the retrievals originate from the most similar neighboring track pixel. If no similar pixel is found, the parameters are fill values. Please refer to the description of the IIR Level 2 Track data product for the description of the track parameters.

Table of Contents

Glossary and Acronym Dictionary

Term	Meaning
AFWA	U.S. Air Force Weather Agency
$ß_{eff}$	microphysical index
CALIOP	Cloud-Aerosol Lidar with Orthogonal Polarization
CALIPSO	Cloud-Aerosol Lidar and Infrared Pathfinder Satellite Observation
D_e	effective diameter
GEOS	Goddard Earth Observing System
granule	continuous data segment in which all measurements were acquired while the lidar was configured for daytime data acquisition only or nighttime data acquisition only; each granule spans approximately one half of a full orbit, with daytime granules being slightly larger/longer than nighttime granules
HDF	Hierarchical Data Format
IAB	Integrated Attenuated Backscatter
IGPB	International Geosphere–Biosphere Programme
IIR	Imaging Infrared Radiometer
LEM	Low Energy Mitigation
LUT	Look-Up Table
MERRA-2	Modern-Era Retrospective Analysis for Research and Applications, Version 2
N/A	Not Applicable
QA	quality assurance/quality control
SDS	Scientific Data Set
TAI	International Atomic Time
UTC	Coordinated Universal Time
WFC	Wide Field of view Camera
WRS	Worldwide Reference System

Additional documentation

Project Documentation

- CALIPSO Data Management Team: CALIPSO Data Products Catalog, PC-SCI-503, Release 5.00.
- Pelon, J., A. Garnier, O. Chomette, M. Viollier, P. Dubuisson, V. Giraud, F. Parol, S. A. Ackerman, D. P. Kratz, Y. Hu, and M. R. Platt, CALIPSO IIR Algorithm Theoretical Basis Document, Level 2 data products, PC-SCI-204, https://ntrs.nasa.gov/citations/20250008391.

Peer-Reviewed Algorithm Papers

- Dubuisson, P., V. Giraud, O. Chomette, H. Chepfer, and J. Pelon, 2005*:* Fast radiative transfer modeling for infrared imaging radiometry. *J. Quant. Spectrosc. Radiat. Transfer*, ***95***, 201–220, https://doi.org/10.1016/j.jqsrt.2004.09.034.

- Dubuisson, P., V. Giraud, J. Pelon, B. Cadet, and P. Yang, 2008: Sensitivity of Thermal Infrared Radiation at the Top of the Atmosphere and the Surface to Ice Cloud Microphysics, *J. Appl. Meteor. Climatol.*, **47**, 2545–2560, https://doi.org/10.1175/2008JAMC1805.1.
- Garnier, A., J. Pelon, P. Dubuisson, M. Faivre, O. Chomette, N. Pascal and D. P. Kratz, 2012: Retrieval of cloud properties using CALIPSO Imaging Infrared Radiometer. Part I: effective emissivity and optical depth, *J. Appl. Meteor. Climatol.*, **51**, 1407–1425, https://doi.org/10.1175/JAMC-D-11-0220.1.
- Garnier, A., J. Pelon, P. Dubuisson, P. Yang, M. Faivre, O. Chomette, N. Pascal, P. Lucker and T. Murray, 2013: Retrieval of cloud properties using CALIPSO Imaging Infrared Radiometer. Part II: effective diameter and ice water path, *J. Appl. Meteor. Climatol.,* **52**, 2582–2599, https://doi.org/10.1175/JAMC-D-12-0328.1.
- Mitchell, D. L., A. Garnier, J. Pelon and E. Erfani, 2018: CALIPSO (IIR-CALIOP) Retrievals of Cirrus Cloud Ice Particle Concentrations, *Atmos. Chem. Phys.*, **18**, 17325–17354, https://doi.org/10.5194/acp-18-17325-2018.
- Garnier, A., J. Pelon, N. Pascal, M. A. Vaughan, P. Dubuisson, P. Yang and D. L. Mitchell, 2021a: Version 4 CALIPSO IIR ice and liquid water cloud microphysical properties, Part I: the retrieval algorithms, *Atmos. Meas. Tech.*, **14**, 3253–3276, https://doi.org/10.5194/amt-14-3253-2021.
- Garnier, A., J. Pelon, N. Pascal, M. A. Vaughan, P. Dubuisson, P. Yang and D. L. Mitchell, 2021b: Version 4 CALIPSO IIR ice and liquid water cloud microphysical properties, Part II: results over oceans, *Atmos. Meas. Tech.*, **14**, 3277–3299, https://doi.org/10.5194/amt-14-3277-2021.
- Mitchell, D. L., A. Garnier, and S. Woods, 2025: Advances in CALIPSO (IIR) cirrus cloud property retrievals – Part 1: Methods and testing, *Atmos. Chem. Phys.*, **25**, 14071–14098, https://doi.org/10.5194/acp-25-14071-2025.

Data Product Descriptions

Latitude

Units: degrees_north

Format: Float_32

Valid Range: -90.0, 90.0

Fill Value: -9999.0

Description: Geodetic latitude at the center of the pixel, duplicate of the Latitude parameter in the Level 1B IIR product.

Longitude

Units: degrees_east

Format: Float_32

Valid Range: -180.0, 180.0

Fill Value: -9999.0

Description: Longitude at the center of the pixel, duplicate of the Longitude parameter in the Level 1B IIR product.

LIDAR_Shot_Time

Units: TAI seconds

Format: Float_64

Valid Range: 4.204E8, 9.623E8

Fill Value: -9999.0

Description: Duplicate of the Lidar_Shot_Time from the similar track pixel in the IIR Level 2 track product based on the homogeneity index. International Atomic Time (TAI) in elapsed seconds from January 1, 1993.

IIR_Track_Pixel_ID

Units: NoUnits

Format: Int_16

Valid Range: 1, 22000

Fill Value: -9999

Description: Identification number of the track pixel in the IIR Level 2 track product similar to the current pixel based on the homogeneity index. IIR_Track_Pixel_ID is 1 for the first record of the track product and is incremented by 1 for the following pixels up to "nb_pixels" for the last record, where "nb_pixels" is the number of pixels in the track file. The pixels at the center of the 69-km swath (i.e. in column 35 when columns are counted from 1 to 69) are the track pixels and have themselves as similar track pixels if there is co-located lidar data (i.e. Type of Scene ≠ -99). Otherwise, these track pixels are treated as swath no-track pixels. IIR_Track_Pixel_ID can be used to extract any track parameter not already reported in the swath product. Fill values indicate that no similar track pixels were found.

IIR_Image_Time_12_05

Units: TAI seconds

Format: Float_64

Valid Range: 4.204E8, 9.623E8

Fill Value: -9999.0

Description: Duplicate of the Image_Time_12.05 in the Level 1B IIR product. International Atomic Time (TAI) in elapsed seconds from January 1, 1993.

LIDAR_DayNight_Flag

Units: NoUnits

Format: Int_8

Valid Range: 0, 1

Fill Value: -99

Description: Lighting conditions at an altitude of ~24 km above mean sea level taken from the CALIOP Level 2 layer product; 0=daytime, 1=nighttime.

Brightness_Temperature_08_65

Brightness_Temperature_12_05

Brightness_Temperature_10_60

Units: K

Format: Int_16

Valid Range: 0.0, 400.0

Fill Value: -9999

Scale Factor: 100.0

Offset: 100.0

Scale Equation: data/scale_factor + offset

Description: Brightness temperature for IIR channel 8.65, 12.05 and 10.6 calculated from the corresponding IIR Level 1B calibrated radiance using the equation and the coefficients given in Sect. 2.4 of Garnier et al. (2018).

Calibrated_WFC_Reflectance

Units: NoUnits

Format: Int_16

Valid Range: 0.0, 2.0

Fill Value: -9999

Scale Factor: 10000.0

Offset: 0.0

Scale Equation: data/scale_factor + offset

Description: Duplicate of the Reflectance parameter from the WFC IIR Level 1B product.

Surface_Emissivity_08_65

Surface_Emissivity_12_05

Surface_Emissivity_10_60

Units: NoUnits

Format: Int_16

Valid Range: 0.0, 1.0

Fill Value: -9999

Scale Factor: 1000.0

Offset: 0.0

Scale Equation: data/scale_factor + offset

Description: Surface emissivity for IIR channel 8.65, 12.05 and 10.6 for the similar track pixel in the IIR Level 2 track product based on the homogeneity index.

Effective_Emissivity_08_65

Effective_Emissivity_12_05

Effective_Emissivity_10_60

Units: NoUnits

Format: Int_16

Valid Range: 0.0, 1.0

Fill Value: -9999

Scale Factor: 1000.0

Offset: 0.0

Scale Equation: data/scale_factor + offset

Description: Effective emissivity for IIR channel 8.65, 12.05 and 10.6 for the similar track pixel in the IIR Level 2 track product based on the homogeneity index.

Effective_Emissivity_Uncertainty_08_65

Effective_Emissivity_Uncertainty_12_05

Effective_Emissivity_Uncertainty_10_60

Units: NoUnits

Format: Int_16

Valid Range: 0.0, 1.0

Fill Value: -9999

Scale Factor: 1000.0

Offset: 0.0

Scale Equation: data/scale_factor + offset

Description: Effective emissivity uncertainty for IIR channel 8.65, 12.05 and 10.6 for the similar track pixel in the IIR Level 2 track product based on the homogeneity index.

Homogeneity_Index_BT_08_65

Homogeneity_Index_BT_12_05

Homogeneity_Index_BT_10_60

Units: NoUnits

Format: Int_8

Valid_Range: 0.0, 1.0

Fill Value: -99

Scale Factor: 100.0

Offset: 0.0

Scale Equation: data/scale_factor + offset

Description: For each IIR channel, absolute difference between the brightness temperature of the current pixel and the brightness temperature of the most similar neighboring (within +/- 100 km) track pixel, varying between 0 (identical temperatures) and 1, which corresponds to the maximum accepted difference of 1 K. If the difference is larger than 1K, this index is set to a fill value. For track pixels with co-located lidar data (i.e. Type of Scene ≠ -99), this index is equal to 0. Track pixels with no co-located lidar data are treated as swath no-track pixels.

Homogeneity_Index_Surface_e_08_65

Homogeneity_Index_Surface_e_12_05

Homogeneity_Index_Surface_e_10_60

Units: NoUnits

Format: Int_8

Valid_Range: 0.0, 1.0

Fill Value: -99

Description: Not reported for this release, set to a fill value.

Homogeneity_Reflectance

Units: NoUnits

Format: Int_8

Valid_Range: 0.0, 1.0

Fill Value: -99

Description: Not reported for this release, set to a fill value.

Homogeneity_Surface_Temperature

Units: NoUnits

Format: Int_8

Valid_Range: 0.0, 1.0

Fill Value: -99

Description: Not reported for this release, set to a fill value.

Homogeneity_Humidity_Profile

Units: NoUnits

Format: Int_8

Valid_Range: 0.0, 1.0

Fill Value: -99

Description: Not reported for this release, set to a fill value.

Particle_Shape_Index

Units: NoUnits

Format: Int_8

Valid Range: 1, 9

Fill Value: -99

Description: Particle shape index retrieved for the similar track pixel in the IIR Level 2 track product based on the homogeneity index.

Particle_Shape_Confidence

Units: NoUnits

Format: Int_8

Valid Range: 1, 4

Fill Value: -99

Description: Particle shape index confidence for the similar track pixel in the IIR Level 2 track product based on the homogeneity index.

Effective_Particle_Size

Units: µm

Format: Int_16

Valid Range: 0.0, 200.0

Fill Value: -9999

Scale Factor: 100.0

Offset: 0.0

Scale Equation: data/scale_factor + offset

Description: Effective particle diameter retrieved for the similar track pixel in the IIR Level 2 track product based on the homogeneity index.

Effective_Particle_Size_Uncertainty

Units: µm

Format: Int_16

Valid Range: 0.0, 200.0

Fill Value: -9999

Scale Factor: 10.0

Offset: 0.0

Scale Equation: data/scale_factor + offset

Description: Effective particle diameter uncertainty estimate for the similar track pixel in the IIR Level 2 track product based on the homogeneity index.

Optical_Depth_12_05

Units: NoUnits

Format: Int_16

Valid Range: 0.0, 10.0

Fill Value: -9999

Scale Factor: 1000.0

Offset: 0.0

Scale Equation: data/scale_factor + offset

Description: Effective absorption optical depth at IIR channel 12.05 retrieved for the similar track pixel in the IIR Level 2 track product based on the homogeneity index.

Optical_Depth_12_05_Uncertainty

Units: NoUnits

Format: Int_16

Valid Range: 0.0, 10.0

Fill Value: -9999

Scale Factor: 1000.0

Offset: 0.0

Scale Equation: data/scale_factor + offset

Description: Estimated uncertainty in the effective absorption optical depth at IIR channel 12.05 for the similar track pixel in the IIR Level 2 track product based on the homogeneity index.

Liquid_Water_Path

Units: g/(m^2)

Format: Int_16

Valid Range: 0.0, 1300.0

Fill Value: -9999

Scale Factor: 30.0

Offset: 20.0

Scale Equation: data/scale_factor + offset

Description: Ice or liquid water path reported for the similar track pixel in the IIR Level 2 track product based on the homogeneity index.

Liquid_Water_Path_Confidence

Units: g/(m^2)

Format: Int_16

Valid Range: 0.0, 1300.0

Fill Value: -9999

Scale Factor: 30.0

Offset: 20.0

Scale Equation: data/scale_factor + offset

Description: Estimated uncertainty in the ice or liquid water path for the similar track pixel in the IIR Level 2 track product based on the homogeneity index.

Integrated_Water_Vapor_Path

Units: g/(cm^2)

Format: Int_16

Valid Range: 0.0,10.0

Fill Value: -9999

Scale Factor: 100.0

Offset: 0.0

Scale Equation: data/scale_factor + offset

Description: Column-integrated atmospheric water vapor path associated to the similar track pixel in the IIR Level 2 track product based on the homogeneity index. This parameter is provided only for some values of Type of Scene. For the missing scenes, it can be extracted from the track product using IIR_Track_Pixel_ID.

Scene_Flag

Units: NoUnits

Format: Int_32

Valid Range: 10010,180099

Fill Value: -9999

Scale Factor: 100.0

Offset: 0.0

Scale Equation: TGeotype = Integer(data/scale_factor) and Type_of_Scene = data - TGeotype * scale_factor

Description: This parameter is a composite of two track parameters for the similar track pixel in the IIR Level 2 track product based on the homogeneity index.

Table 1: Interpretation of Scene Flag

Digits	Interpretation
Tens-Units	Type_of_Scene
Hundreds of thousands to Hundreds	TGeotype

IIR_Data_Quality_Flag

Units: NoUnits

Format: Int_8

Valid Range: 0, 15

Fill Value: -99

Description: Indicator of the IIR calibrated radiance quality extracted from the Pixel_Quality_Index of the IIR Level 1B product. If not zero, corresponding to nominal quality:

- either one channel has poor quality or is missing, or
- the radiances in the 3 channels are not all part of the same image measurement sequences which, for scenes with high broken clouds, could lead to some errors at the edge of the images for geometrical reasons.

Table 2: Interpretation of IIR Data Quality Flag

Bit	Bit Value	Interpretation
1	0	IIR calibrated radiances in the 3 channels are of nominal quality
	1	At least one of the channels has poor quality or is missing
2	0	Channels 08.65 and 10.60 derived from the same sequence of acquisition
	1	Channels 08.65 and 10.60 not derived from the same sequence of acquisition
3	0	Channels 08.65 and 12.05 derived from the same sequence of acquisition
	1	Channels 08.65 and 12.05 not derived from the same sequence of acquisition
4	0	Channels 10.60 and 12.05 derived from the same sequence of acquisition
	1	Channels 10.60 and 12.05 not derived from the same sequence of acquisition
5-8	N/A	N/A

Equalization_Flag

Units: NoUnits

Format: Int_8

Valid Range: 0, 7

Fill Value: -99

Description: Indicator of whether an equalization correction has been applied, extracted from the Pixel_Quality_Index of the IIR Level 1B product.

Table 3: Interpretation of Equalization Flag

Bit	Bit Value	Interpretation Equalization Correction
1	0	Channel 12.05: no
	1	Channel 12.05: yes
2	0	Channel 10.60: no
	1	Channel 10.60: yes
3	0	Channel 08.65: no
	1	Channel 08.65: yes

Bit	Bit Value	Interpretation Equalization Correction
4-8	N/A	N/A

Layer_Top_Height_Upper_Level

Units: km

Format: Int_16

Valid Range: -0.5, 30.1

Fill Value: -9999

Scale Factor: 1000.0

Offset: 0.0

Scale Equation: data/scale_factor + offset

Description: Layer_Top_Height_Upper_Level parameter for the similar track pixel in the IIR Level 2 track product based on the homogeneity index.

Centroid_IAB_0532_Upper_Level

Units: km

Format: Int_16

Valid Range: -0.5, 30.1

Fill Value: -9999

Scale Factor: 1000.0

Offset: 0.0

Scale Equation: data/scale_factor + offset

Description: Centroid_IAB_0532_Upper_Level parameter for the similar track pixel in the IIR Level 2 track product based on the homogeneity index.

Layer_Bottom_Height_Upper_Level

Units: km

Format: Int_16

Valid Range: -0.5, 30.1

Fill Value: -9999

Scale Factor: 1000.0

Offset: 0.0

Scale Equation: data/scale_factor + offset

Description: Layer_Bottom_Height_Upper_Level parameter for the similar track pixel in the IIR Level 2 track product based on the homogeneity index.

Layer_Top_Temperature_Upper_Level

Units: K

Format: Int_16

Valid Range: 160.0, 340.0

Fill Value: -9999

Scale Factor: 100.0

Offset: 100.0

Scale Equation: data/scale_factor + offset

Description: Layer_Top_Temperature_Upper_Level parameter for the similar track pixel in the IIR Level 2 track product based on the homogeneity index.

Temperature_Centroid_IAB_0532_Upper_Level

Units: K

Format: Int_16

Valid Range: 160.0, 340.0

Fill Value: -9999

Scale Factor: 100.0

Offset: 100.0

Scale Equation: data/scale_factor + offset

Description: Temperature_Centroid_IAB_0532_Upper_Level parameter for the similar track pixel in the IIR Level 2 track product based on the homogeneity index.

Layer_Bottom_Temperature_Upper_Level

Units: K

Format: Int_16

Valid Range: 160.0, 340.0

Fill Value: -9999

Scale Factor: 100.0

Offset: 100.0

Scale Equation: data/scale_factor + offset

Description: Layer_Bottom_Temperature_Upper_Level parameter for the similar track pixel in the IIR Level 2 track product based on the homogeneity index.

Layer_Top_Pressure_Upper_Level

Units: hPa

Format: Int_16

Valid Range: 1.0, 1086.0

Fill Value: -9999

Scale Factor: 10.0

Offset: 0.0

Scale Equation: data/scale_factor + offset

Description: Layer_Top_Pressure_Upper_Level parameter for the similar track pixel in the IIR Level 2 track product based on the homogeneity index.

Pressure_Centroid_IAB_0532_Upper_Level

Units: hPa

Format: Int_16

Valid Range: 1.0, 1086.0

Fill Value: -9999

Scale Factor: 10.0

Offset: 0.0

Scale Equation: data/scale_factor + offset

Description: Pressure_Centroid_IAB_0532_Upper_Level parameter for the similar track pixel in the IIR Level 2 track product based on the homogeneity index.

Layer_Bottom_Pressure_Upper_Level

Units: hPa

Format: Int_16

Valid Range: 1.0, 1086.0

Fill Value: -9999

Scale Factor: 10.0

Offset: 0.0

Scale Equation: data/scale_factor + offset

Description: Layer_Bottom_Pressure_Upper_Level parameter for the similar track pixel in the IIR Level 2 track product based on the homogeneity index.

Layer_Top_Height_Lower_Level

Units: km

Format: Int_16

Valid Range: -0.5, 30.1

Fill Value: -9999

Scale Factor: 1000.0

Offset: 0.0

Scale Equation: data/scale_factor + offset

Description: Layer_Top_Height_Upper_Level parameter for the similar track pixel in the IIR Level 2 track product based on the homogeneity index.

Centroid_IAB_0532_Lower_Level

Units: km

Format: Int_16

Valid Range: -0.5, 30.1

Fill Value: -9999

Scale Factor: 1000.0

Offset: 0.0

Scale Equation: data/scale_factor + offset

Description: Centroid_IAB_0532_Lower_Level parameter for the similar track pixel in the IIR Level 2 track product based on the homogeneity index.

Layer_Bottom_Height_Lower_Level

Units: km

Format: Int_16

Valid Range: -0.5, 30.1

Fill Value: -9999

Scale Factor: 1000.0

Offset: 0.0

Scale Equation: data/scale_factor + offset

Description: Layer_Bottom_Height_Lower_Level parameter for the similar track pixel in the IIR Level 2 track product based on the homogeneity index.

Layer_Top_Temperature_Lower_Level

Units: K

Format: Int_16

Valid Range: 160.0, 340.0

Fill Value: -9999

Scale Factor: 100.0

Offset: 100.0

Scale Equation: data/scale_factor + offset

Description: Layer_Top_Temperature_Lower_Level parameter for the similar track pixel in the IIR Level 2 track product based on the homogeneity index.

Temperature_Centroid_IAB_0532_Lower_Level

Units: K

Format: Int_16

Valid Range: 160.0, 340.0

Fill Value: -9999

Scale Factor: 100.0

Offset: 100.0

Scale Equation: data/scale_factor + offset

Description: Temperature_Centroid_IAB_0532_Lower_Level parameter for the similar track pixel in the IIR Level 2 track product based on the homogeneity index.

Layer_Bottom_Temperature_Lower_Level

Units: K

Format: Int_16

Valid Range: 160.0, 340.0

Fill Value: -9999

Scale Factor: 100.0

Offset: 100.0

Scale Equation: data/scale_factor + offset

Description: Layer_Bottom_Temperature_Lower_Level parameter for the similar track pixel in the IIR Level 2 track product based on the homogeneity index.

Layer_Top_Pressure_Lower_Level

Units: hPa

Format: Int_16

Valid Range: 1.0, 1086.0

Fill Value: -9999

Scale Factor: 10.0

Offset: 0.0

Scale Equation: data/scale_factor + offset

Description: Layer_Top_Pressure_Lower_Level parameter for the similar track pixel in the IIR Level 2 track product based on the homogeneity index.

Pressure_Centroid_IAB_0532_Lower_Level

Units: hPa

Format: Int_16

Valid Range: 1.0, 1086.0

Fill Value: -9999

Scale Factor: 10.0

Offset: 0.0

Scale Equation: data/scale_factor + offset

Description: Pressure_Centroid_IAB_0532_Lower_Level parameter for the similar track pixel in the IIR Level 2 track product based on the homogeneity index.

Layer_Bottom_Pressure_Lower_Level

Units: hPa

Format: Int_16

Valid Range: 1.0, 1086.0

Fill Value: -9999

Scale Factor: 10.0

Offset: 0.0

Scale Equation: data/scale_factor + offset

Description: Layer_Bottom_Pressure_Lower_Level parameter for the similar track pixel in the IIR Level 2 track product based on the homogeneity index.

Metadata Parameter Descriptions

Product_ID

An 80-byte character string containing the product name. For the IIR Level 2 swath products, the value of this string is "CAL_IIR_L2_Swath".

Date_Time_at_Granule_Start

A 27-byte character string that specifies the granule start date and time. The format is yyyy-mm-ddThh:nn:ss.ffffffZ, where yyyy is the year, mm is the month, dd is the day, hh is the hour, nn is the minute, ss is the second, and ffffff is the fractional second. Date and time are separated by the character 'T'. The 'Z' indicates that time is given in UTC.

Date_Time_at_Granule_End

A 27-byte character string that specifies the granule end date and time. The format is yyyy-mm-ddThh:nn:ss.ffffffZ, where yyyy is the year, mm is the month, dd is the day, hh is the hour, nn is the minute, ss is the second, and ffffff is the fractional second. Date and time are separated by the character 'T'. The 'Z' indicates that time is given in UTC.

Date_Time_of_Production

A 27-byte character string that specifies the date and time at granule production. The format is yyyy-mm-ddThh:nn:ss.ffffffZ, where yyyy is the year, mm is the month, dd is the day, hh is the hour, nn is the minute, ss is the second, and ffffff is the fractional second. Date and time are separated by the character 'T'. The 'Z' indicates that time is given in UTC.

Initial_IIR_Scan_Center_Latitude

This field reports the first subsatellite latitude of the granule.

Initial_IIR_Scan_Center_Longitude

This field reports the first subsatellite longitude of the granule.

Ending_IIR_Scan_Center_Latitude

This field reports the last subsatellite latitude of the granule.

Ending_IIR_Scan_Center_Longitude

This field reports the last subsatellite longitude of the granule.

Orbit_Number_at_Granule_Start

Orbit_Number_at_Granule_Stop

Orbit_Number_Change_Time

Orbit Number consists of three fields that define the number of revolutions by the CALIPSO spacecraft around the Earth. This number is incremented each time the spacecraft passes the equator on the ascending node. To maintain consistency between the CALIPSO and CloudSat orbit parameters, the Orbit Number is keyed to the CloudSat orbit 2121 at 23:00:47 on 2006/09/20. Because the CALIPSO data granules are organized according to the day and night conditions, based on fixed Sun-Earth-Satellite angles, day/night boundaries do not coincide with transition points for defining orbit number. As such, three parameters are needed to describe the orbit number for each granule as:

- **Orbit Number at Granule Start:** orbit number at the granule start time.
- **Orbit Number at Granule End:** orbit number at the granule stop time.
- **Orbit Number Change Time:** time at which the orbit number changes in the granule.

Path_Number_at_Granule_Start

Path_Number_at_Granule_Stop

Path_Number_Change_Time

Path Number consists of three fields that define an index ranging from 1-233 that references orbits to the Worldwide Reference System (WRS). This global grid system was developed to support scene identification for LandSat imagery. Since the A-Train is maintained to the WRS grid within +/- 10 km, the Path Number provides a convenient index to support data searches, instead of having to define complex latitude and longitude regions along the orbit track. The Path Number is incremented after the maximum latitude in the orbit is attained and changes by a value of 16 between successive orbits. Because the CALIPSO data granules are organized according to the day and night conditions, based on fixed Sun-Earth-Satellite angles, day/night boundaries do not coincide with transition points for defining path number. As such, three parameters are needed to describe the path number for each granule as:

- **Path Number at Granule Start:** path number at the granule start time.
- **Path Number at Granule End:** path number at the granule stop time.
- **Path Number Change Time:** time at which the path number changes in the granule.

While CALIPSO was formation flying in the A-Train all path numbers in the metadata are exact. Beginning in September 2018, when CALIPSO lowered its orbit into the C-Train, path numbers are no longer exact, but they instead indicate the closest WRS reference orbit.

Number_of_IIR_Records_in_File

Number of 69-km records in the file.

Number_of_Valid_08_65_Pixels

Number of pixels in the file with valid radiance in IIR channel 8.65.

Number_of_Valid_12_05_Pixels

Number of pixels in the file with valid radiance in IIR channel 12.05.

Number_of_Valid_10_60_Pixels

Number of pixels in the file with valid radiance in IIR channel 10.6.

Number_of_Invalid_08_65_Pixels

Number of pixels in the file with invalid radiance in IIR channel 8.65.

Number_of_Invalid_12_05_Pixels

Number of pixels in the file with invalid radiance in IIR channel 12.05.

Number_of_Invalid_10_60_Pixels

Number of pixels in the file with invalid radiance in IIR channel 10.6.

Number_of_Rejected_08_65_Pixels

Number of IIR pixels in the file in channel 8.65 rejected by the algorithm because no similar track pixel was found.

Number_of_Rejected_12_05_Pixels

Number of IIR pixels in the file in channel 12.05 rejected by the algorithm because no similar track pixel was found.

Number_of_Rejected_10_60_Pixels

Number of IIR pixels in the file in channel 10.6 rejected by the algorithm because no similar track pixel was found.

Number_of_Rejected_08_65_Pixels_Location

This field is set to -9999.

Number_of_Rejected_12_05_Pixels_Location

This field is set to –9999.

Number_of_Rejected_10_60_Pixels_Location

This field is set to –9999.

Number_of_Rejected_08_65_Pixels_Rad

This field is set to –9999.

Number_of_Rejected_12_05_Pixels_Rad

This field is set to –9999.

Number_of_Rejected_10_60_Pixels_Rad

This field is set to –9999.

Mean_08_65_Radiance_All

Mean radiance (in W/((m^2)·sr·µm)) in the file in IIR channel 8.65 for the non-rejected pixels.

Mean_12_05_Radiance_All

Mean radiance (in W/((m^2)·sr·µm)) in the file in IIR channel 12.05 for the non-rejected pixels.

Mean_10_60_Radiance_All

Mean radiance (in W/((m^2)·sr·µm)) in the file in IIR channel 10.6 for the non-rejected pixels.

Mean_08_65_Radiance_Selected_Cases

Mean radiance (in W/((m^2)·sr·µm)) in the file in IIR channel 8.65 for the cases selected for emissivity retrievals.

Mean_12_05_Radiance_Selected_Cases

Mean radiance (in W/((m^2)·sr·µm)) in the file in IIR channel 12.05 for the cases selected for emissivity retrievals.

Mean_10_60_Radiance_Selected_Cases

Mean radiance (in W/((m^2)·sr·µm)) in the file in IIR channel 10.6 for the cases selected for emissivity retrievals.

Mean_08_65_Brightness_Temp_All

Mean brightness temperature (in Kelvin) in the file in IIR channel 8.65 for non-rejected pixels.

Mean_12_05_Brightness_Temp_All

Mean brightness temperature (in Kelvin) in the file in IIR channel 12.05 for non-rejected pixels.

Mean_10_60_Brightness_Temp_All

Mean brightness temperature (in Kelvin) in the file in IIR channel 10.6 for non-rejected pixels.

Mean_08_65_Brightness_Temp_Selected_Cases

Mean brightness temperature (in Kelvin) in the file in IIR channel 8.65 for the cases selected for emissivity retrievals.

Mean_12_05_Brightness_Temp_Selected_Cases

Mean brightness temperature (in Kelvin) in the file in IIR channel 12.05 for the cases selected for emissivity retrievals.

Mean_10_60_Brightness_Temp_Selected_Cases

Mean brightness temperature (in Kelvin) in the file in IIR channel 10.6 for the cases selected for emissivity retrievals.

GEOS_Version

Specifies the version of the meteorological data used in the analyses. For the version 5.0 data release, this field is always “MERRA2”.

Data Release Information

Table 4: Dates, versions, and production strategy for all CALIPSO IIR level 2 data releases

IIR Level 2 Track and Swath, half orbit (Day and Night)			
Release Date	**Version**	**Data Date Range**	**Production Strategy**
October 2025	5.00	June 13, 2006 to June 30, 2023	Standard
October 2023	4.51	June 13, 2006 to June 30, 2023	Standard
October 2020	4.21	July 1, 2020 to January 19, 2022	Standard
April 2020	4.20	June 13, 2006 to June 30, 2020	Standard
October 2020	3.46	October 1, 2020 to June 30, 2023	Beta
September 2018	3.45	September 1, 2018 to September 30, 2020	Beta
December 2016	3.40	December 1, 2016 to August 31, 2018	Beta
August 2013	3.30	March 1, 2013 to November 30, 2016	Beta
December 2011	3.02	November 1, 2011 to February 28, 2013	Beta
May 2011	3.01	June 13, 2006 to October 31, 2011	Beta
October 2008	2.02	September 14, 2008 to January 17, 2011	Beta
October 2008	2.01	June 13, 2006 to September 13, 2008	Beta

Data Quality Information

Data Quality Statement for the release of the CALIPSO IIR Level 2 Product Version 5.00

The IIR level 2 Version 5.00 (V5) algorithm uses the new Version 3.00 IIR level 1B products while the previous IIR level 2 V4.51 algorithm (V4) used the previous Version 2. A new IIR level 1B version was generated to accommodate new code that generated two new public products, namely the IIR Level 1 Calibration and IIR Level 1 Calibration

Correction data products. There was no change to the IIR Level 1B science algorithm and the reported brightness temperatures are identical in IIR level 2 V5 and V4 data products.

For this V5 data release, the suitable types of scenes for IIR retrievals are classified using the V5 CALIOP 5-km Cloud and Aerosol 5-km layer products. We recall that the retrievals are applied to the so-called *upper level* which includes either one single semi-transparent or opaque layer, or several semi-transparent layers. The V5 algorithm uses for the first time the temperature and extinction profiles reported in the V5 CALIOP cloud profile product to improve radiative temperature estimates and to produce a new series of retrievals when the *upper level* is composed of semi-transparent ice clouds (new parameter names starting with "Cirrus").

The main algorithm changes implemented in V5 are in the track algorithm. They are listed below and are then described and assessed in more details:

- Changes related to the CALIOP Low Energy Mitigation algorithm implemented in the CALIOP V5 level 2 products,
- Adjustments related to the surface emissivity and surface temperature correction maps,
- Addition of the radiative temperature of the *upper level* with improved estimates in transparent ice clouds,
- Addition of radiative height and pressure associated with radiative temperature of the *upper level*,
- Addition of cloud optical depth and estimated uncertainty,
- Addition of a suite of new "cirrus" retrievals in transparent ice clouds and estimated uncertainties.

Changes related to the CALIOP Low Energy Mitigation algorithm

Over the last seven years of the mission, the CALIOP laser experienced an increasing frequency of shots with low to zero energy, which were initially prevailingly located over the South Atlantic Anomaly and were then observed more globally at the end of the mission. A low energy mitigation (LEM) algorithm (Tackett et al., 2025) is implemented in the CALIOP Level 2 V5 products, which identifies level 1 backscatter data resulting from low energy pulses and, when appropriate, excludes it from the level 2 analyses. The CALIOP Low_Energy_Mitigation_Column_QC_Flag parameter, which summarizes the operation of the LEM algorithm within each 5 km vertical column in the CALIOP profile products, is duplicated in the IIR track product.

As in the previous versions, the scenes with lidar data that do not match the prescribed classification are reported as Type_of_Scene = 99. For this version 5.00 data release, the IIR pixels in 5-km columns that are rejected by the LEM algorithm fall into that category. The 5-km columns including low energy shots and accepted by the LEM algorithm are considered of nominal quality. The Low_Energy_Mitigation_Column_QC_Flag parameter can be used for further quality filtering if deemed necessary.

In V4, the "Was_Cleared_Flag_1km" parameter reported the number of clouds seen by the 1-km IIR pixel that were detected by CALIOP at single shot resolution and that were cleared from the CALIOP 5-km layer products (noted *number_cleared_shots*). In V5, Was_Cleared_Flag_1km contains also the number of single shot profiles seen by the 1-km IIR pixel that were rejected by the LEM algorithm (noted *number_rejected_profiles*). This flag is now built as:

Was_Cleared_Flag_1km = 10 x *number_rejected_profiles* + *number_cleared_shots*

Both *number_cleared_shots* and *number_rejected_profiles* are between 0 and 3 and their sum is necessarily smaller than or equal to 3. When no single shot profiles were rejected by LEM, the interpretation of the flag is unchanged compared to V4. As in V4, the cloud-free (clear sky or aerosol only) scenes must have Was_Cleared_Flag_1km = 0. Indeed, scenes having Was_Cleared_Flag_1km = 10, 20, or 30 have 1 to 3 single-shot profiles rejected by the LEM algorithm and the presence of small-scale cloud(s) is unknown. Similarly, it is recommended, as in V4, to ensure that Was_Cleared_Flag_1km = 0 for detailed analyses of retrievals in optically thin clouds.

Surface emissivity and surface temperature corrections maps

The monthly maps (resolution: latitude x longitude = 1° x 2°) of surface emissivity at 8.65 and 10.6 µm and of surface temperature correction introduced in V4 were augmented near the coasts to account for orbital drifts after CALIPSO joined the C-Train in October 2018. The new coastal values were derived using neighboring pixels over land. In addition, a small inaccuracy of the latitude and longitude values used to read the maps was fixed in V5. This caused a pixel located at the border of two grid cells to be possibly assigned a wrong set of surface values. Overall, after these changes, less than 0.2 % of the pixels are assigned different surface parameters in V5 and in V4.

Radiative temperature of the *upper level* with improved estimates in transparent ice clouds

The radiative temperature of the upper level is the temperature used to compute the top of atmosphere blackbody brightness temperature at 12.05 µm, which is required to retrieve the effective emissivity of the *upper level* at 12.05 µm. Even though it could be retrieved by the user from Temperature_Centroid_IAB_0532_Upper_Level augmented by the difference between the 6th and 3rd records of the Blackbody_Brightness_Temperature parameter, it is now reported for clarity.

In V4, this temperature was derived from the V4 parameterized functions described in Section 3.4.2 of Garnier et al. (2021a) when the upper level was composed of ice clouds. Otherwise, this temperature was Temperature_Centroid_IAB_0532_Upper_Level.

For this V5 release, when the upper level is composed of semi-transparent ice clouds, this temperature corresponds to the radiance obtained from equation 5 in Garnier et al. (2021a), where the in-cloud temperature and extinction profiles are from the CALIOP V5 cloud profile product. This equation was used to determine the V4 parameterized functions, and it is instead now applied for each sample. Figure 1 compares the V4.51 and the V5 radiative temperatures for the month of April 2010 and statistics are given in Table 5. Both retrievals are in good agreement overall, with a larger dispersion for multi-layer upper levels for which both the initial estimate of the centroid temperature and the V4 parameterized functions could yield larger errors than in single-layer cases.

Table 5: Statistical analysis of V5-V4.51 radiative temperature differences (in Kelvin) in semi-transparent icy single-layer and multi-layer *upper levels*. April 2010.

	Night		Day	
	Mean	**Standard deviation**	**Mean**	**Standard deviation**
Single-layer	0.06	0.84	0.21	0.65
Multi-layer	0.39	2.5	0.57	2.7

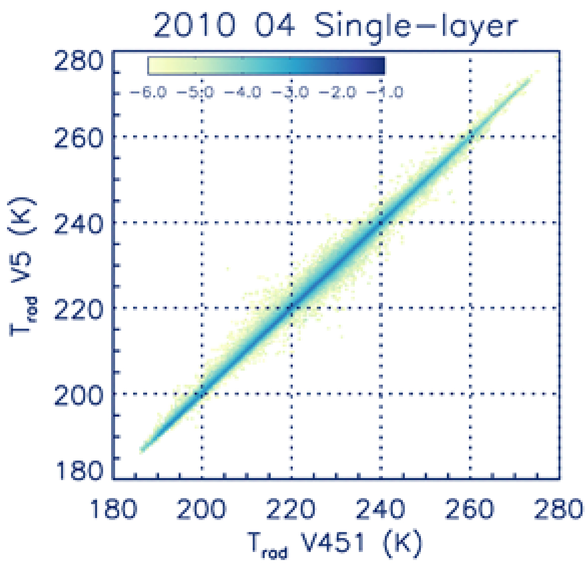

Figure 1: Comparison of V5 (Y-axis) and V4.51 (X-axis) radiative temperatures of upper levels composed of semi-transparent ice clouds for single-layer (left) and multi-layer (right) upper levels. The colors indicate the normalized number of samples in logarithm

Radiative height and pressure of the *upper level*

Radiative height and pressure corresponding to the radiative temperature of the *upper level* are now reported.

Cloud optical depth and estimated uncertainty

The V5 track product now includes cloud visible optical depth as retrieved by IIR when the *upper level* includes only ice clouds or only water clouds. For ice clouds, cloud optical depth is derived from effective emissivity at 10.6 and 12.05 µm using equation 11b in Garnier et al. (2021a). For water clouds, cloud optical depth varies with retrieved effective diameter (see equations 12 and 13a-b in Garnier et al., 2021a) and could be retrieved by the user from liquid water path and absorption optical depth at 12.05 µm. Cloud optical depth is provided in V5 for more clarity, and the estimated uncertainty is now available.

Suite of new "cirrus" retrievals in transparent ice clouds and estimated uncertainties

This V5 data release includes a new series of retrievals when the *upper level* is composed of semi-transparent ice clouds (new parameter names starting with "Cirrus").

"Cirrus" optical and microphysical properties are retrieved using new analytical functions relating the $ß_{eff}$12/10 microphysical index and various microphysical quantities derived from in situ measurements at tropical and mid-latitudes performed during the TC4, ATTREX, POSIDON, and SPARTICUS field experiments. These retrievals are detailed in Mitchell et al. (2025) where the analytical functions are shown in Table 3 and the strategy to combine them as a function of latitude and radiative temperature is summarized in Table 5.

The algorithm uses CALIOP in-cloud temperature and extinction profiles to estimate the equivalent layer thickness seen by IIR, which represents 30 to 90 % of the layer geometrical thickness (see section 6.1 in Garnier et al., 2021a and section 2.2.5 in Mitchell et al., 2025). This IIR equivalent thickness is used to retrieve the layer "vertically resolved" quantities, namely layer ice number concentration, layer extinction, and layer ice water content.

Both cirrus optical depth (Cirrus_Optical_Depth) and standard optical depth (Cloud_Optical_Depth) are derived using relationships between effective absorption efficiency at 12 µm ($Q_{abs,eff}$(12 µm)) and $ß_{eff}$12/10 microphysical index. For standard optical depth (COD), the retrieval equation is COD = $\tau_{a,10} + \tau_{a,12}$ where $\tau_{a,10}$ and $\tau_{a,12}$ are the effective absorption depths at 10.6 µm and 12.05 µm, respectively. This yields $1/Q_{abs,eff}$ (12 µm) = 0.5 x (1+ 1/ $ß_{eff}12/10$) when taking visible extinction = 2 as also assumed for the cirrus retrievals.

Figure 2 compares the standard and cirrus optical depth retrievals for the month of April 2010. The [standard – cirrus] relative optical depth difference is 9 % on average with a standard deviation of 13 %.

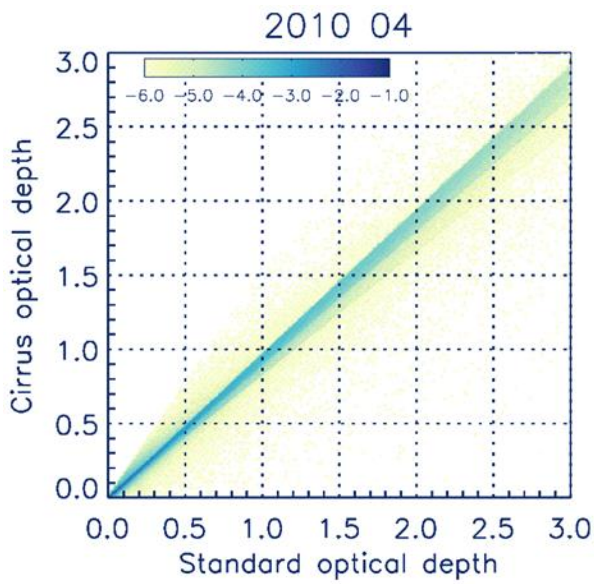

Figure 2: Comparison of cirrus (Y-axis) and standard (X-axis) optical depths of upper levels composed of semi-transparent ice clouds. The colors indicate the normalized number of samples in logarithm scale. April 2010.

Cirrus effective diameter (D_e) (Cirrus_Effective_Diameter) differs from standard D_e (Effective_Particle_Size) whose retrieval is based on various look-up tables assuming gamma particle size distributions and where both $ß_{eff}12/10$ and $ß_{eff}12/08$ microphysical indices are used to select the ice crystal model and ultimately produce D_e (Garnier et al., 2021a). Figure 3 shows cirrus D_e vs. standard D_e for single-layer columns over oceans where the particle shape index confidence parameter indicates confident standard retrievals. The horizontal lines at cirrus D_e = 77.5, 136.5 and 129.5 µm correspond to samples having $ß_{eff}12/10$ smaller than the sensitivity limits of each of the 3 cirrus formulations below which D_e cannot be retrieved and is set to this maximum value. They correspond to standard D_e primarily between 60 and 120 µm.

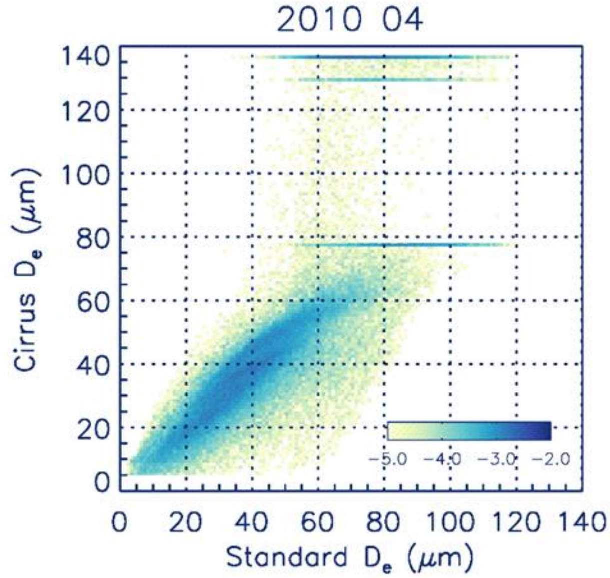

Figure 3: Comparison of cirrus (Y-axis) and standard (X-axis) effective diameters for single-layer semi-transparent ice columns over oceans and confident standard retrievals. The colors indicate the normalized number of samples in logarithm scale. April 2010.

Update Format of CALIPSO HDF Files

The V5.00 IIR Level 2 data products are distributed as Hierarchical Data Format Version 4 (HDF4) files, consistent with the EOS requirement in effect when CALIPSO launched in 2006. Since launch, there have been substantial technological advances in data discoverability and access resources. To make this data more readily accessible to the scientific community beyond the life of the mission and take advantage of newer data access capabilities, several modifications were made to the look and format of the WFC HDF files. These include:

- Update all units to conform to NetCDF Climate and Forecast (CF) metadata conventions.
- Verify all dimensions are named, to allow HDF to NCDF conversions using commercial off the shelf (COTS) tools that currently exist.
- Create/expand attributes and comments for all SDSs to make the data products more self-documenting.

Data Quality Statement for the release of the CALIPSO IIR Level 2 Product Version 4.51

The V4 IIR Level 2 algorithm, described in details in Garnier et al. (2021a, 2021b), takes full advantage of the co-located characterization of the atmosphere provided by CALIOP. The same V4 algorithm was used to generate these new V4.51 data products and the previous V4.2 data products. In V4.51, the V4 algorithm is applied to suitable types of scenes classified using the V4.51 CALIOP 5-km Cloud and Aerosol layer products, whereas the previous V4.2 data products were derived from the previous V4.2x CALIOP data products. The retrievals are applied to the so-called *upper level* which includes either one single semi-transparent or opaque layer, or several semi-transparent layers.

Data Quality Statement for the release of the CALIPSO IIR Level 2 Product Version 4.21

A minor version bump (+0.01) has been applied to all CALIPSO data products due to a required upgrade to the operating system on the CALIPSO production cluster. All algorithms were re-compiled to process in this new environment with no change to the underlying science algorithms or inputs.

Data Quality Statement for the release of the CALIPSO IIR Level 2 Product Version 4.20

The IIR Level 2 algorithm, described in details in Garnier et al. (2012, 2013), takes full advantage of the co-located characterization of the atmosphere provided by CALIOP. It is applied to suitable types of scenes classified using the V4.20 CALIOP 5-km Cloud and Aerosol layer products. The retrievals are applied to the so-called *upper level* cloud which includes either one single semi-transparent or opaque layer, or several semi-transparent layers.

Effective emissivity retrievals require i) a correction for the contribution from the "background" and ii) the determination of the radiative temperature of the *upper level* cloud. When the lowermost of at least two individual cloud layers in the column is opaque to CALIOP, the background reference is from this opaque layer, which is called *lower level*. Otherwise, the background reference is from the Earth surface in clear air conditions. Both in the older V3 and in V4, the first step into the computation of the radiative temperature is to determine the centroid altitude of the *upper level* cloud.

As in V3, ice cloud effective diameter (D_e) retrievals use the concept of microphysical index ($ß_{eff}$) applied to the IIR pairs of channels (12.05, 10.6) and (12.05, 8.65), with $ß_{eff}$12/10 and $ß_{eff}$12/08 defined as the 12.05-to-10.6 and 12.05-to-08.65 ratios of the effective absorption optical depths, respectively. The microphysical indices are interpreted in terms of D_e by using Look-Up Tables (LUTs) built for several models. The ice water path is then determined from calculated effective emissivities and D_e.

The most significant changes in the V4 algorithm with respect to V3 include:

- A refined scene classification
- An updated radiative transfer model analysis for clear air reference with new surface emissivity values and corrected land surface temperature
- A revised centroid altitude in multi-layer cases
- Refined radiative temperature estimates in ice clouds
- Updated and extended microphysical retrievals in ice clouds
- Addition of microphysical retrievals in liquid water clouds
- Revised uncertainty estimates

Refined Scene Classification

Was_Cleared_Flag_1km

In V4, a new "Was_Cleared_Flag_1km" parameter reports the number of clouds seen by the 1-km IIR pixel that were detected by CALIOP at single shot resolution and that were cleared from the CALIOP 5-km layer products. These clouds have a top altitude < 4 km. In V3, these single-shot cleared clouds were not reported in the CALIOP 5-km layer products and they were ignored by the IIR algorithm.

In V4, the cloud-free (clear sky or aerosol only) scenes must have Was_Cleared_Flag_1km = 0. When Was_Cleared_Flag_1km ≠ 0, these scenes, which were thought to be cloud-free in V3, are assigned new types of scenes in V4.

For effective emissivity retrievals, the background radiance is computed regardless of Was_Cleared_Flag_1km. Unless the bias in the background radiance due to the cleared clouds can be estimated a posteriori and can be deemed acceptable, it is recommended to ensure that Was_Cleared_Flag_1km = 0 for detailed analyses of retrievals in optically thin clouds.

Absorbing Aerosols

For the scenes that fall into the "clouds" category, the semi-transparent aerosol layers, if any, are ignored when computing the cloud effective emissivity. In V4, we require that the "clouds" scenes that contain only one or two semi-transparent cloud layers do not contain high (typically stratospheric) aerosol layers, because these high aerosol layers could absorb in the IIR channels.

In addition, the presence of potentially absorbing aerosol layers (i.e. tropospheric dust or stratospheric aerosols) is now reported in a new Dust_Stratospheric_Aerosol_Flag and a new Dust_Stratospheric_Aerosol_Flag_QA so that the retrievals can be filtered using these flags.

Updated Radiative Transfer Model Analysis for Clear Air Reference

When no relevant neighboring observations can be found, the background reference is computed using a radiative transfer model, meteorological profiles and surface temperature from MERRA-2 re-analyses, and surface emissivity values.

Model

The radiative transfer model has been updated in V4 to better simulate absorption by water vapor.

Surface Category, Surface Emissivity, and Surface Temperature

In V3, the surface emissivity values in each IIR channel were theoretical static values assigned to each IGBP Surface Type. When the daily Snow_Ice_Surface_type indicated the presence of snow or sea ice, IGBP Surface Type was changed to IGBP = 15 (snow/ice).

In V4, the characterization of the surface has been refined, and is reported in a new "TGeotype" parameter. TGeotype is assigned using IGBP Surface Type and the co-located Surface_532_Integrated_Depolarization_Ratio, now reported in the V4 CALIOP products, and Snow_Ice_Surface_type if Surface_532_Integrated_Depolarization_Ratio is not available. Surface_532_Integrated_Depolarization_Ratio is also used to refine the land/water classification around coastlines. The TGeotype values fall into five main categories: water, water/sea ice transition, sea ice, snow, and snow-free land.

Surface emissivity values used in V4 have been determined empirically from the analysis of two years of IIR data in clear sky conditions. The V4 algorithm continues to use static values for the water, water/sea ice transition, sea ice, and snow categories. For the snow-free land category, the V3 static values per IGBP type at 08.65 µm and 10.6 µm are replaced with monthly daytime and nighttime maps (resolution: latitude x longitude = 1° x 2°), while a constant value (0.975) is taken at 12.05 µm. In case of snow-free land, the surface temperature is the initial MERRA 2 surface temperature further corrected using monthly daytime and nighttime correction maps that were derived using the 12.05 µm reference channel by reconciling calculations and IIR observations.

Summary of Clear Air Reference Changes from V3 to V4

The changes described above improve the accuracy of effective emissivity and microphysical retrievals in optically thin layers when the clear air background radiance is derived from the model. Subsequently, retrievals derived from observed and computed background radiances are more consistent in V4 than in V3.

Over oceans, the change from V3 to V4 is for the most part the reduction of systematic effective emissivity biases at 08.65 µm, which improves the reliability of effective diameter retrievals. Even though less accurate than over oceans, retrievals over land are improved in V4, in particular in desertic areas and in polar regions.

Revised Centroid Altitude in Multi-layer Cases

Because of an error in the V3 algorithm, the centroid altitude of multi-layer systems could be too low by up to 3 km in V3. This has been fixed in V4.

Refined Radiative Temperature Estimates in Ice Clouds

In V3, the radiative temperature was set to the temperature at the lidar centroid altitude for any cloud or aerosol system. The approach is the same in V4, except when all the layers are classified as ice by the V4 CALIOP ice/water phase algorithm. In the latter case, the initial centroid temperature estimate (which was used in V3) has been shown to be too cold (Garnier et al., 2015). It is now refined in V4 using parameterized correction functions. Blackbody brightness temperatures derived from both the centroid temperature and the V4 radiative temperature are reported in the V4 product.

The correction applied in V4 has a negligible impact on effective emissivity values smaller than about 0.3. The largest impact is for opaque clouds, the correction being more efficient for nighttime than for daytime data. For instance, for oceanic opaque ice clouds in January 2008, nighttime and daytime distributions of effective emissivity at 12.05 µm peak respectively at 0.99 and 0.97 in V4, compared to 0.94 in V3.

Updated Microphysical Retrievals in Ice Clouds

Optical Properties

The three ice crystal models used in V3 have been replaced with two ice crystal models in V4, namely severely rough "single hexagonal column" and "8-element column aggregate" elaborated from new ice properties (Yang et al., 2013; Bi and Yang, 2017). In addition, a gamma particle size distribution with effective variance equal to 0.1 is taken in V4, whereas there was no size distribution in V3. As a result of these changes, De is increased from V3 to V4.

Four independent sets of De derived from a second approach are also reported in V4. This approach uses analytical functions relating ßeff12/10 and De as derived from in situ measurements at tropical and mid-latitudes performed during the TC4 and SPARTICUS field experiments (Mitchell et al., 2018).

Ice Water Path

For ice clouds, Ice Water Path is estimated from De and visible extinction optical depth (τ_{vis}) derived from calculated effective emissivities. In V3, τ_{vis} was approximated to $2\tau_{a,12}$, where $\tau_{a,12}$ is the IIR affective absorption optical depth at 12.05 µm. In V4, τ_{vis} is approximated to $\tau_{a,12} + \tau_{a,10}$, where $\tau_{a,10}$ is the IIR affective absorption optical depth at 10.6 µm. The V4 approximate reduces the dependence on D_e and improves the τ_{vis} estimate by up 10 % for D_e > 20 µm.

Addition of Microphysical Retrievals in Liquid Water Clouds

Unlike in V3, microphysical retrievals in liquid water clouds are provided in V4.

For D_e retrievals, the LUTs are computed using the Mie theory with refractive indices from Hale and Querry (1973) and again using a gamma particle size distribution (PSD) with effective variance equal to 0.1. No temperature dependence of infrared absorption is included.

Liquid Water Path is estimated from D_e, $\tau_{a,12}$, and $Q_{a,12}(D_e)$, where the latter is the effective absorption efficiency at 12.05 µm, whose variation with $D_e \leq 20$ µm is represented using a fourth-degree polynomial. In agreement with

Pinnick et al. (1979), $Q_{a,12}$ increases quasi-linearly with D_e < 10 µm up to about 1, and then increases slowly up to 1.15 as D_e increases from 10 to 20 µm.

Revised Uncertainty Estimates

For each IIR channel, the estimated uncertainty in the effective emissivity is composed of three terms associated to

- an error dT_m in the measured brightness temperature,
- an error dT_{BG} in the background reference brightness temperature,
- an error dT_{BB} in the blackbody temperature.

In V3, the reported uncertainties were computed using $dT_m = dT_{BG} = dT_{BB} = 1$ K. Table 6 describes the temperature errors used in V4.

Table 6: Contributions to the Estimated Effective Emissivity Uncertainties Based on Surface

	Water Surface	Non-Water Surface
dT_m(K)	0.3	0.3
dT_{BG}(K)	1	3
dT_{BB}(K)	2	2

In V4, the three terms used to compute the estimated uncertainty in the effective emissivity are reported.

Effective Diameter Uncertainty

The approach chosen to report the estimated uncertainty in D_e has been changed in V4. In V4, it is simply inferred from the estimated uncertainty in the microphysical indices and from the LUT used for the retrievals.

Ice or Liquid Water Path Uncertainty

Unlike in V3, an estimated uncertainty in the ice or liquid water path is reported in V4. It is computed from the estimated uncertainty in D_e and in the effective absorption optical depth(s).

Data Quality Statement for the release of the CALIPSO IIR Level 2 Product Version 3.46

A minor version bump (+0.01) has been applied to all CALIPSO data products due to a required upgrade to the operating system on the CALIPSO production cluster. All algorithms were re-compiled to process in this new environment with no change to the underlying science algorithms or inputs.

Data Quality Statement for the release of the CALIPSO IIR Level 2 Product Version 3.45

All CALIPSO science data executables were migrated to a new production cluster. Because of the need to make minor algorithm changes and recompile, the version number of the IIR Level 2 data products has changed from V3.40 to V3.45. All other data products successfully transferred without the need to recompile and retain their existing versioning.

Data Quality Statement for the release of the CALIPSO IIR Level 2 Product Version 3.40

Version 3.40 data products reflect a transition of the Global Modeling and Assimilation Office (GMAO) Forward Processing – Instrument Teams (FP-IT) meteorological data version from 5.9.1 to 5.12.4.

Data Quality Statement for the release of the CALIPSO IIR Level 2 Product Version 3.30

Version 3.30 data products incorporate the updated GMAO Forward Processing - Instrument Teams (FP-IT) meteorological data, and the enhanced Air Force Weather Authority (AFWA) Snow and Ice Data Set as ancillary inputs to the production of these data sets, beginning with data date March 1, 2013.

Impacts on CALIOP data products, of which IIR Level 2 use as input, caused by the transition to GEOS-5 FP-IT are predicted to be minimal, based on a comparison of CALIOP Version 3.02 against CALIOP Version 3.30.

IIR Level 2 algorithm uses ancillary surface and atmospheric data to compute background and blackbody radiances before retrieving effective emissivity and optical depth.

In case of cirrus clouds over ocean, absorption optical depth derived from computed background radiances is predicted to change by less than 0.01 on average between 60S and 60N, and to be more accurate in V3.30. These predictions are inferred from distributions of brightness temperature (BT) differences between observations and computations in clear sky conditions over ocean for several ranges of latitude in August 2013 (V3.30), which have been compared to distributions for the months of August 2012 and 2010 (V3.02 and V3.01, respectively). The mean BT differences are reduced by 0.1 to 0.3 Kelvin in absolute value in V3.30, with similar standard deviations (1.2 and 1.9 Kelvin). At high latitude, a more accurate identification of the IIR pixels not impacted by snow or ice results into smaller standard deviations in V3.30. No significant change of the computed blackbody radiances has been identified for opaque ice clouds for the month of August 2013.

In case of cirrus clouds overlying a low opaque cloud, changes in absorption optical depth derived from computed background radiances are predicted from distributions of differences between observations and computations for low opaque clouds. The median BT differences are improved by 0.4 to 1.2 Kelvin in August 2013 (V3.30) compared to August 2010 and 2012, corresponding to changes of the order of 0.01 to 0.03 in absorption optical depth.

Data Quality Statement for the release of the CALIPSO IIR Level 2 Product Version 3.02

Version 3.02 reflects a change in the data products due to a required upgrade to the operating system on the CALIPSO production cluster. All algorithms were re-compiled to process in this new environment with no change to the underlying science algorithms or inputs

Data Quality Statement for the release of the CALIPSO IIR Level 2 Product Version 3.01

Version 3.01 includes microphysical parameters which were not available in Version 2: effective particle size and uncertainty, particle shape and confidence, and ice-water path. The optical depth derived from the effective emissivity at 12.05 µm has been added.

Version 3.01 IIR scene classification algorithm has been updated with respect to Version 2 (cf Type of Scene, IIR/Lidar track product). Also, Version 3.01 IIR products use Version 3.01 CALIOP Level 2 products (instead of Version 2 for the previous release). Overall, changes in the IIR scene classification are significant in Version 3.01 compared to Version 2.

Data Quality Statement for the release of the CALIPSO IIR Level 2 Product Version 2.20

N/A

Data Quality Statement for the release of the CALIPSO IIR Level 2 Product Version 2.01

N/A

References

Bi, L. and P. Yang, 2017: Improved ice particle optical property simulations in the ultraviolet to far-infrared regime, *J. Quant. Spectrosc. Radiat. Transfer*, **189**, 228–237, https://doi.org/10.1016/j.jqsrt.2016.12.007.

Garnier, A., J. Pelon, M. A. Vaughan, D. M. Winker, C. R. Trepte, and P. Dubuisson, 2015: Lidar multiple scattering factors inferred from CALIPSO lidar and IIR retrievals of semi-transparent cirrus cloud optical depths over oceans, *Atmos. Meas. Tech.*, **8**, 2759–2774, https://doi.org/10.5194/amt-8-2759-2015.

Garnier, A., T. Trémas, J. Pelon, K.-P. Lee, D. Nobileau, L. Gross-Colzy, N. Pascal, P. Ferrage, and N. A. Scott, 2018: CALIPSO IIR Version 2 Level 1b calibrated radiances: analysis and reduction of residual biases in the Northern Hemisphere, *Atmos. Meas. Tech.*, **11**, 2485–2500, https://doi.org/10.5194/amt-11-2485-2018.

Hale, G. M. and M. R. Querry, 1973: Optical constants of water in the 200 nm to 200 µm wavelength region, *Appl. Opt.*, **12**, 555–563, https://doi.org/10.1364/AO.12.000555.

Parol, F., J. C. Buriez, G. Brogniez, and Y. Fouquart,1991: Information content of AVHRR channels 4 and 5 with respect to the effective radius of cirrus cloud particles, *J. Appl. Meteor.*, **30**, 973–984, https://doi.org/10.1175/1520-0450-30.7.973.

Pinnick, R. G., S. G. Jennings, P. Chylek, and H. J. Auvermann, 1979: Verification of a linear relation between IR extinction, absorption and liquid water content of fogs, *J. Atmos. Sci.*, **36**, 1577–1586, https://doi.org/10.1175/1520-0469(1979)036<1577:VOALRB>2.0.CO;2.

Tackett, J. L., R. A. Ryan, A. E. Garnier, J. Kar, B. Getzewich, X. Cai, M. A. Vaughan, C. R. Trepte, R. Verhappen, D. M. Winker, and K.-P. A. Lee, 2025: Mitigating impacts of low energy laser pulses on CALIOP data products, *Atmos. Meas. Tech.*, **18**, 6211–6231, https://doi.org/10.5194/amt-18-6211-2025.

Yang, P., H. Wei, H. L. Huang, B. A. Baum, Y. X. Hu, G. W. Kattawar, M. I. Mishchenko, and Q. Fu, 2005: Scattering and absorption property database for non-spherical ice particles in the near-through far-infrared spectral region, *Appl. Opt.*, **44**, 5512–5523, https://doi.org/10.1364/AO.44.005512.

Yang, P., L. Bi, B. A. Baum, K.-N. Liou, G. W. Kattawar, M. I. Mishchenko, and B. Cole, 2013: Spectrally consistent scattering, absorption, and polarization properties of atmospheric ice crystals at wavelengths from 0.2 µm to 100 µm, *J. Atmos. Sci.*, **70**, 330–347, https://doi.org/10.1175/JAS-D-12-039.1.